HHS Public Access

Author manuscript

Cytotherapy. Author manuscript; available in PMC 2016 June 21.

Published in final edited form as:

Cytotherapy. 2015 May ; 17(5): 579–592. doi:10.1016/j.jcyt.2014.12.003.

Notch ligand Delta-like 1 promotes *in vivo* vasculogenesis in human cord blood–derived endothelial colony forming cells

HYOJIN KIM[1,2,3,4], **LAN HUANG**[1,2,3,*], **PAUL J. CRITSER**[1,2], **ZHENYUN YANG**[1,2], **REBECCA J. CHAN**[1,2], **LIN WANG**[1,2,5], **NADIA CARLESSO**[1,2,5], **SHERRY L. VOYTIK-HARBIN**[6], **IRWIN D. BERNSTEIN**[4], and **MERVIN C. YODER**[1,2,3]

[1]Department of Pediatrics, Indiana University School of Medicine, Indianapolis, Indiana, USA

[2]Herman B. Wells Center for Pediatric Research, Indiana University School of Medicine, Indianapolis, Indiana, USA

[3]Department of Biochemistry and Molecular Biology, Indiana University School of Medicine, Indianapolis, Indiana, USA

[4]Fred Hutchinson Cancer Research Center, Seattle, Washington, USA

[5]Department of Medical and Molecular Genetics, Indiana University School of Medicine, Indianapolis, Indiana, USA

[6]Weldon School of Biomedical Engineering, Purdue University, West Lafayette, Indiana, USA

Abstract

Background aims—Human cord blood (CB) is enriched in circulating endothelial colony forming cells (ECFCs) that display high proliferative potential and *in vivo* vessel forming ability. Because Notch signaling is critical for embryonic blood vessel formation *in utero*, we hypothesized that Notch pathway activation may enhance cultured ECFC vasculogenic properties *in vivo*.

Methods—*In vitro* ECFC stimulation with an immobilized chimeric Notch ligand (Delta-like1$^{ext\text{-}IgG}$) led to significant increases in the mRNA and protein levels of Notch regulated Hey2 and EphrinB2 that were blocked by treatment with γ-secretase inhibitor addition. However, Notch stimulated preconditioning *in vitro* failed to enhance ECFC vasculogenesis *in vivo*. In contrast, *in vivo* co-implantation of ECFCs with OP9-Delta-like 1 stromal cells that constitutively expressed the Notch ligand delta-like 1 resulted in enhanced Notch activated ECFC-derived increased vessel density and enlarged vessel area *in vivo*, an effect not induced by OP9 control stromal implantation.

Correspondence: **Mervin C. Yoder**, MD, Wells Center for Pediatric Research, 1044 W. Walnut Street, R4-W125, Indianapolis, IN 46202. myoder@iu.edu.

*These authors contributed equally to this work.

Disclosure of interest: The authors have no commercial, proprietary, or financial interest in the products or companies described in this article.

Supplementary data

Supplementary data related to this article can be found at http://dx.doi.org/10.1016/j.jcyt.2014.12.003.

Results—This Notch activation was associated with diminished apoptosis in the exposed ECFC.

Conclusions—We conclude that Notch pathway activation in ECFC *in vivo* via co-implanted stromal cells expressing delta-like 1 promotes vasculogenesis and augments blood vessel formation via diminishing apoptosis of the implanted ECFC.

Keywords

apoptosis; endothelial colony forming cells (ECFCs); Notch ligand delta-like 1 (Dll1); OP9-Delta-like 1 stromal cells (OP9-DL1); vasculogenesis

Introduction

The Notch signaling pathway is an evolutionarily conserved pathway that is involved in a variety of developmental processes [1–3]. Notch family members and Notch ligands are expressed in endothelial cells (ECs) throughout early vascular development [4–6]. Notch 1, Notch 4, Jagged 2, delta-like 1 (Dll1) and 4 (Dll4) are specifically expressed in arterial endothelium [5,7], and these molecules play critical roles in arterial specification [8–13]. Vascular endothelial growth factor (VEGF) is one of the most potent and ubiquitous vascular growth factors that affect many aspects of EC biology. Recently, VEGF-A has been found to interact with the activated Notch pathway to determine and maintain arterial EC fate [13–15]. Less is known of how Notch signaling may influence the vasculogenic properties of human vessel forming cells.

In Notch 1– and 4–deficient mouse embryos, embryos failed to remodel the plexus to form large and small blood vessels, although the primary vascular plexus appeared to form normally. This indicates that Notch signaling plays a critical role in angiogenic vascular morphogenesis and remodeling [16,17]. Different human EC lines have been studied the regulation of Notch signaling pathway in human vascular development. Most studies have used human umbilical vein endothelial cells (HUVECs) or human arterial/microvascular endothelial cells to investigate the roles of the Notch signaling pathway on their angiogenic and vasculogenic behavior. Notch 1 activation has been implicated both in promoting and in inhibiting cell death in a cell type specific manner [18–21]. Notch 1 activation in cultured monocytes plated upon immobilized $Delta^{ext\text{-}myc}$ has been reported to induce apoptosis [22]. On the other hand, activation of Notch 1 and a downstream mediator, HES1, in human iliac artery endothelial cells (HIAECs) caused growth suppression but improved cell survival of the cultured cells. Also, activated Notch 1 in HIAECs formed more stabilized network and cord formation on Matrigel substrate in the presence of VEGF [23]. Dll1-dependent Notch signaling mediated by Ephrin-B2 induced branching morphogenesis and network formation by human arterial endothelial cells (HAECs) plated on Matrigel [24]. These reports indicated that Notch 1 signaling plays a role in regulating endothelial cell survival and network and cord formation *in vitro*, but limited evidence has been presented to examine how *in vitro* Notch activation preconditioning might influence angiogenic or vasculogenic behavior when cells are implanted *in vivo*.

We have successfully isolated circulating endothelial colony forming cells (ECFCs) from human umbilical cord blood (CB) and identified a hierarchy of proliferative potential in ECFC through the use of single-cell clonogenic and functional assays [25,26]. Human CB ECFCs form a human capillary plexus in immunodeficient mice after subcutaneous implantation in collagen-fibronectin gels and, upon inosculation with murine vessels, become a part of the systemic host circulation [26,27]. We have recently determined that all viable circulating ECFCs in human CB and adult peripheral blood can be enriched and identified as ECs expressing CD34, CD146, CD105 and CD31, but not CD45 or CD133 [28]. These circulating viable endothelial cells represent those rare circulating ECFC that are known to colonize and re-endothealize implanted biomaterials in human subjects [29,30].

The use of circulating CB ECFCs to study human vessel formation within immunodeficient mice permits analysis of human vasculogenesis and determination of key regulatory molecules controlling human vessel formation *in vivo* in a unique model system. For example, use of cultured CB ECFC with adult bone marrow mesenchymal stromal cells (MSCs) can re-create a hematopoietic and leukemic stem cell niche *in vivo* [31]. Because Notch pathway activation plays such a key role in establishing the murine embryonic vascular system, we hypothesized that *in vitro* preconditioning of human CB ECFC with Notch ligand may enhance *in vivo* vasculogenic activity. We report that preconditioning of ECFC with Notch activation *in vitro* is insufficient to promote *in vivo* vasculogenesis; however, provision of the Notch ligand Dll1 by OP9 stromal cells *in vivo* activates Notch 1 signaling in ECFC and enhances human blood vessel formation.

Methods

Media and supplements

Human Endothelial serum free medium (Invitrogen) was supplemented with 20 ng/mL human recombinant basic fibroblast growth factor (Invitrogen), 10 ng/mL human recombinant epidermal growth factor (R&D), 10 ng/mL human recombinant vascular endothelial growth factor 165 (rhVEGF-A/rhVEGF$_{165}$; R&D), 10 ng/mL rhVEGF$_{121}$ (R&D), 10 ng/mL stem cell factor (R&D), 5 ng/mL stromal cell–derived factor 1alpha (R&D), 10 ng/mL interleukin 6 (IL6) (R&D) and 1.5% human cord plasma, to create serum reduced medium (SRM).

Isolation and culture of human umbilical CB–derived ECFCs

Human umbilical CB samples (50–100 mL) were collected in heparin-coated syringes from healthy newborns (38–40 weeks' gestation). The Institutional Review Board at Indiana University School of Medicine reviewed and approved this study with exempt status. Umbilical CB was diluted 1:1 with Dulbecco's phosphate-buffered saline (PBS) (Invitrogen) and overlaid onto Ficoll-Paque PLUS (GE Healthcare). Cells were centrifuged for 30 min at room temperature at 1500 rpm. Mononuclear cells (MNCs) were isolated and washed with Dulbecco's PBS. For outgrowth of ECFC colonies, MNCs were resuspended in SRM; 3×10^7 MNCs were seeded onto each well of 6-well tissue culture plates pre-coated with type I rat-tail collagen (BD Biosciences Pharmingen) and cultured as previously described [25]. ECFC colonies appeared at ~4 days of culture and were noted to form colonies of adherent cells

with cobblestone morphology. After ~10 days of culture, the ECFC-derived ECs were released from the culture dish by TrypLE Express (Gibco) and replated onto 25-cm^2 tissue culture flasks pre-coated with type I rat-tail collagen for subsequent passage. Characterization of human umbilical CB ECFC–derived ECs was conducted using monoclonal antibodies and fluorescence-activated cell sorter analysis as previously described [25].

Immobilization of Delta1$^{ext\text{-}IgG}$ protein

Delta1$^{ext\text{-}IgG}$ protein is the extracellular domain of human Dll1 fused to the Fc domain of human immunoglobulin (Ig)G1 [32]. Non-tissue culture-treated plates were coated with decreasing concentrations of Delta1$^{ext\text{-}IgG}$ (20, 10, 5, 2.5, 1.25, 0.625 and 0.3125 μg/mL) or the same concentration of human IgG (Sigma-Aldrich), diluted in PBS together with 5 μg/mL fibronectin fragment CH-296 (Takara Shuzo). The plates were incubated overnight at 4°C, washed with PBS 3 times and further incubated with 2% bovine serum albumin dissolved in PBS at 37°C for 1 h. Thereafter, plates were washed with PBS 3 times and were then ready for plating cells.

RNA isolation and conventional/quantitative reverse transcriptase polymerase chain reaction

Total cellular RNA was extracted with an RNeasy Micro extraction kit (Qiagen) as described by the manufacturer. Reverse transcriptase (RT) reactions were performed using an Omniscript RT Kit (Qiagen). Conventional polymerase chain reaction (PCR) was conducted by using Go Tap Flexi DNA Polymerase (Promega) according to the manufacturer's instructions. The primer sequences are shown in Table I. The PCR cycle profile was 94°C for 5 min; 94°C for 30 s, 53 or 57°C (depending on the different primers) for 30 s, 72°C for 45 s, and 32 cycles with a final 72°C for 7 min. PCR products were added to wells in a 2% agarose/ethidium bromide gel and exposed to electrophoresis current. Migrating bands were photographed under ultraviolet light.

Quantitative PCR was performed using FastStart Universal SYBR green master 2× (Rox) (Roche). The relative standard curve of each gene amplification was first generated to determine the amplification efficiency (Eff). ATP5B was used as a housekeeping gene. To compare gene expression levels among treated and control ECFCs, results were presented as the ratio of the expression of each gene to ATP5B expression. For Delta1$^{ext\text{-}IgG}$ or γ-secretase inhibitor L685 458 treatment effects on ECFCs, gene expression levels in non-treated cells at day 0 were analyzed as controls. Results were expressed as a fold change (in logarithmic scale) compared with the control. The quantitative analysis was performed according to Pfaffl's method [33]. The primer sequences are shown in Table II.

Notch ligand and receptor cell surface expression on ECFCs

Relative levels of Notch ligands and receptors on ECFCs were determined by flow cytometry. ECFCs were harvested by cell dissociation buffer enzyme-free Hanks'-based reagent (Gibco). Cells (0.5×10^6) were suspended in staining buffer (PBS, 0.5% bovine serum albumin, and 2 mmol/L EDTA) and stained using purified anti-human Notch 4 (clone MHN4-2, BioLegend), biotinylated anti-human Notch 1 (clone mN1A, BioLegend), anti-

human Dll1 conjugated to phycoerythrin (PE) (clone MHD 1–314, BioLegend), anti-human Delta-like protein 4 (Dll4) conjugated to allophycocyanin (APC) (clone MHD 4–46, Bio-Legend) and anti-human CD31 antibody conjugated to PE-Cyanine7 (clone WM-59, eBiosciences) for 15 min at room temperature in the dark. After staining with purified and biotin conjugated primary antibodies, cells were stained with secondary antibody, goat anti-mouse Alexa Fluor 488 (Invitrogen), Streptavidin-APC (eBiosciences) and with propidium iodide (PI) (eBiosciences) for 15 min at room temperature in the dark. For negative controls, we used fluorescence minus 1 (FMO) analysis, as we have previously described [28]. Stained cells were analyzed by FlowJo software.

Western blot

Protein extracts were prepared as described previously [34], electrophoresed using sodium dodecyl sulfate–polyacrylamide gel electrophoresis, transferred to nitrocellulose and probed with anti-human Coup TFII (clone H7147, R&D), anti-human Hey2 (ab167280Abcam) and anti-human β-actin (mAbcam 8226, Abcam). For Notch receptors, proteins were transferred to immobilon-P membrane, PVDF, 0.45 μm (Millipore), and probed with anti-human Notch 1 (clone C-20, Santa Cruz Biotechnology), anti-human Notch 2 (clone 25–255, Santa Cruz Biotechnology) and anti-human Notch 4 (clone H-225, Santa Cruz Biotechnology).

Implantation of human CB–derived ECFCs into NOD/SCID mice

Cellularized gel implants were cast as previously described [26,27]. Cultured ECFCs (2×10^6 cells/mL) were suspended in a solution containing 1.5 mg/mL rat-tail collagen I (BD Biosciences Pharmingen), 100 μg/mL human fibronectin (Chemicon), 1.5 mg/mL sodium bicarbonate (Sigma), 25 mmol/L 4-(-2hydroxyethyl)-1-piperazineethanesulfonic acid (Cambrex), 10% fetal bovine serum, 30% serum free medium, pH-adjusted to 7.4. Then 250 μL of the cell suspension was pipetted into 1 well of a 48-well tissue culture plate, allowed to polymerize at 37°C for 30 min, and covered with 500 μL SRM for overnight incubation at 37°C, in 5% CO_2. Gels were implanted into the flanks of anesthetized 6- to 9-week-old non-obese diabetic (NOD)/severe combined immunodeficient (SCID) mice. After 14 days, the mice were sacrificed; the grafts were excised and analyzed by histology and immunohistochemistry (n = 6) as previously described [26,27]. ECFCs were also co-implanted with OP9 or OP9-DL1 stromal cells in some studies. OP9-DL1 cells represent murine bone marrow stromal OP9 cells that have been engineered to constitutively express the Notch ligand Dll1 [35]. ECFCs and OP9 or OP9-DL1 were implanted at 4:1 ratios as above.

Histology and immunohistochemistry

Sections were stained as previously described [27]. Briefly, paraffin-embedded tissue sections were deparaffinized and then either directly stained with hematoxylin and eosin (H&E) or immersed in retrieval solution (Dako) for 20 min at 90–99°C. Slides were incubated at room temperature for 30 min with anti-human CD31 antibody (clone JC70/A, Abcam), and rat anti-mouse smooth muscle α actin (αSMA) (clone 1A4, Sigma) followed by a 10-minute incubation with LASB2 link-biotin and streptavidin-HRP (Vector Laboratories), then developed with DAB (Vector Laboratories) solution for 5 min. Slides were analyzed by microscope under 40× magnification.

Assessment of apoptosis of ECFCs in 3-dimensional collagen gels

Apoptosis was assessed by examining the percentage of human CD31 positive ECFCs that bound annexin V and propidium iodide and was performed as per the manufacturer's instruction (Apoptosis Detection kit, eBioscience). OP9 or OP9-DL1 cells were co-implanted with ECFCs (1:1) in collagen gels at indicated time points as noted earlier. Collagen gels were prepared as described previously [27,36]. Briefly, 2×10^6 cells/mL were implanted in collagen solution with endothelial cell growth medium (EGM-2, Lonza). Gels were recovered from 1 to 3 days later and incubated in 250 μL Collagenase Type I (0.25%, Stemcell Technology) for 20 min at 37°C. Cell dissociation buffer was added to stop the enzymatic reaction (Invitrogen). Cells were centrifuged at 500 *g* for 5 min at room temperature. Cell pellets were suspended in staining buffer and stained with anti-human CD31 antibody conjugated to PE for 15 min (clone WM-59, BD Biosciences Pharmingen). Cells were incubated in binding buffer for 20 min and stained for Annexin V-APC and PI for 30 min at room temperature in the dark. Stained cells were analyzed by FlowJo software.

Caspase 1 and 3/7 assays in 3-dimensional collagen gels

Relative levels of active caspases 1 and 3/7 activities were determined by flow cytometry using fluorescein-labeled inhibitors of caspases (FLICA) reagent according to the manufacturer's instructions (FLICA 660 caspase 3/7 assay kit and FLICA 660 *in vitro* caspase 1 detection kit, Immunochemistry Technology). Collagen gels and cells were prepared as previously described in assessment of apoptosis above. Cells recovered from gels were suspended in staining buffer and stained with anti-human CD31 antibody conjugated to PE (clone WM-59, BD Biosciences Pharmingen) for 15 min. Cells were incubated with the FLICA 660-DEVD-FMK caspse3/7 inhibitor/FLICA 660-YVAD-FMK caspase 1 inhibitor reagent for 20 min at room temperature in the dark. Unbound reagents were removed by two washes in wash buffer. The cells were stained with PI to assess viability. The cells were analyzed using a LSR II flow cytometer (BD Biosciences Pharmingen) and FlowJo software.

Statistical analysis

Results are expressed as mean ± SEM for the study variables. The change of gene expression after rhVEGF-A, Delta1$^{ext\text{-}IgG}$ or γ-secretase inhibitor L685 458 induction in ECFC was assessed by Student's paired *t*-test. The vessel number and size distribution were evaluated by Student's unpaired *t*-test. A statistically significant difference was set at $P < 0.05$. The quantification of Western blot data points, the number of smooth muscle α actin+ vessels, the assessment of apoptosis of ECFCs, and results of caspase 1 and 3/7 assays in 3-dimensional (3D) collagen gels were assessed by 1-way analysis of variance, $P < 0.05$.

Results

Cultured human CB ECFCs express multiple Notch pathway transcripts

We examined cultured human CB ECFCs to determine if Notch ligand/receptor or downstream genes activated by Notch ligand binding were evident at baseline conditions, along with some typical endothelial transcripts. Cultured ECFCs expressed a variety of the

Notch pathway related transcripts and (Figure 1A). ECFCs displayed several typical endothelial cell surface markers such as platelet endothelial cell adhesion molecule-l (CD31) and vascular endothelial-cadherin (VE-Cad), which are typical of an EC identity and these cells have all been shown to give rise to cultures of ECs that display *in vivo* human vessel forming potential [27,37]. We also demonstrated protein expression of Notch ligands and Notch receptors on ECFCs by flow cytometry (Figure 1B). Although Dll1 was not detected on ECFCs, Notch 1 (2.7 ± 0.5%), Notch 4 (2.9 ± 0.3%) and Dll4 (4.6 ± 0.9%) were expressed on a subset of ECFCs (n = 3).

Delta1$^{ext\text{-}IgG}$ induces known Notch downstream target gene transcripts in human CB ECFCs in a dose-dependent manner

Previous studies have indicated that Notch signaling is required for blood vessel formation during embryo development [4,6,38–40]. In this study, the engineered Notch ligand, Delta1$^{ext\text{-}IgG}$, consisting of the extracellular domain of Dll1 fused to the Fc portion of human IgG, was used to activate Notch signaling in the ECFC. An enzyme-linked immunoabsorbent assay was used to confirm that the concentration of ligand coated on the tissue culture plate surface correlated with the amount of ligand bound as previously described (data not shown) [41]. The linear relationship between the amount of immobilized ligand and activation of Notch signaling was measured by the expression of the Notch downstream target gene Hey2 (Figure 2A,B). After 3 days of culture, cells were harvested and the expression of Hey2 was examined by quantitative PCR. Expression of Hey2 increased as the concentration of Delta1$^{ext\text{-}IgG}$ increased, which indicated that human CB–derived ECFCs were capable of responding to Notch ligand Dll1 stimulation.

We next evaluated whether Delta1$^{ext\text{-}IgG}$ influences other Notch related gene expression patterns in human CB ECFCs. Early passaged [2–4] ECFCs (n = 5) were cultured in wells coated with Delta1$^{ext\text{-}IgG}$ at concentrations ranging from 0.312 to 20 μg/mL or with the same concentration of human IgG as the control attachment ligand. ECFCs displayed a Delta1$^{ext\text{-}IgG}$ dose-dependent increase in Hes1 mRNA expression over 14 days of culture (data not shown), but Dll4, Notch 1 and Notch 4 mRNA were unchanged in the ECFC (online supplementary Figure 1). It is noteworthy that mRNA for the arterial-like endothelial gene markers Hey2 and Ephrin B2 were significantly upregulated after 3 days of Delta1$^{ext\text{-}IgG}$ induction at the concentration of 10 μg/mL (Figure 2B), whereas the expression of mRNAs for the venous-like endothelial gene markers Coup TFII and EphB4 remained at low levels of detection (Figure 2B). Changes in Hey2 and Coup TFII gene expression at the transcript level upon Delta1$^{ext\text{-}IgG}$ binding were confirmed at the protein level (Figure 2C). Immunoblot analysis indicated that the protein level changes of Hey2 and Coup TFII were consistent with their mRNA levels of change. These results demonstrated that Delta1$^{ext\text{-}IgG}$ was able to enhance Notch-related gene expression in human CB ECFCs *in vitro*.

Next, we examined whether Delta1$^{ext\text{-}IgG}$-induced EphrinB2 expression could be suppressed if the Notch signaling pathway was blocked via the use of a γ-secretase inhibitor L685458. The expression of Hes1 and Hey2 mRNA decreased with the addition of the inhibitor to the culture (online supplementary Figure 2A,B). Interestingly, the Delta1$^{ext\text{-}IgG}$-induced

upregulation of mRNA for Hey2 and EphrinB2 was significantly decreased in the presence of 1 μmol/L L685458 for 3 days, whereas the expression of mRNA for Coup TFII was noticeably increased (supplementary Figure 2C). In addition, when control human CB ECFCs were treated with 1 μmol/L L685458 alone for 3 days, the expression of mRNAs for Hey2 and EphrinB2 were dramatically suppressed, whereas the mRNA for Coup TFII was considerably enhanced when compared to Delta$^{ext\text{-}IgG}$ treated cells (supplementary Figure 2C). Collectively, these observations demonstrated that immobilized Dll1 activated Notch signaling is able to regulate ECFC gene expression patterns *in vitro* over several days of exposure.

Dll1 expression by OP9 stromal cells significantly enhances in vivo postnatal vasculogenesis

We subsequently tested whether human CB ECFCs exposed to immobilized Dll1 (Delta1$^{ext\text{-}IgG}$) would increase vasculogenesis after they were implanted *in vivo*. ECFCs were treated with 10 μg/mL of Delta1$^{ext\text{-}IgG}$ for 3 days *in vitro*, then suspended in a collagen-fibronectin matrix and subcutaneously implanted into immunodeficient mice as described [27]. After 14 days, the mice were euthanized, the grafts were harvested, and implants analyzed for blood vessel formation (supplementary Figure 3A). Our data indicated that *in vitro* Delta1$^{ext\text{-}IgG}$-primed human CB ECFCs were unable to enhance vessel formation *in vivo* because the total vascular area of the human vessels was unchanged compared to IgG control cultured cells (supplementary Figure 3B,C). These data indicate that preconditioning of ECFC *in vitro* with Notch activation fails to translate into enhanced vasculogenic properties in ECFC *in vivo*.

Knowing that activation of Notch signaling is mediated by cell–cell interaction between Notch ligands and receptors *in vitro* and *in vivo* [5], we hypothesized that co-implantation of ECFCs with stromal cells constitutively expressing Dll1 may be required to enhance vasculogenesis *in vivo*. ECFCs were cultured in standard conditions and then co-implanted with OP9-Delta-like 1 stromal cells (OP9-DL1) into immunodeficient mice. After 14 days, the mice were euthanized, and the grafts were harvested and investigated for human blood vessel formation. Use of a specific anti-human CD31 antibody revealed that human CB ECFCs were able to form microvessels perfused with murine red blood cells in the grafts (Figure 3A). Of interest, the vessel number and morphology differed between the collagen gel matrices containing ECFC co-implanted with OP9-DL1 (ECFC/OP9-DL1) cells and the control implants (the collagen gels containing ECFC alone or ECFC with OP9 [ECFC/OP9]). The quantification of murine erythrocyte-containing human microvessels (Figure 3B) revealed a significantly greater number of hCD31$^+$ vessels were present in ECFC/OP9-DL1 implants compared with the controls (ECFC alone versus ECFC/OP9 versus ECFC/OP9-DL1 was 30.03 ± 8.14 versus 53.32 ± 7.19 versus 129.10 ± 27.80 vessels/mm^2, respectively, $P < 0.05$). In addition, the size distribution of hCD31$^+$ microvessels was altered with the ECFC/OP9-DL1 implants compared with the control implants (Figure 3C). Noticeably, upon Dll1 stimulation, human CB ECFCs gave rise to significantly more large area microvessels (1000–4000 μm^2) and fewer small ones (51–100 μm^2; Figure 3C). Furthermore, the average vessel area was distinctly increased with the ECFC/OP9-DL1 implants compared to the control implants (Figure 3D, ECFC alone versus ECFC/OP9 versus ECFC/OP9-DL1 was

223.81 ± 15.47 versus 266.03 ± 39.28 versus 384.61 ± 42.73 μm^2, respectively, $P < 0.05$). These alterations resulted in the overall hCD31$^+$ vascular area (= average vessel density × average vessel area) being significantly enhanced in the ECFC/OP9-DL1 implants compared with the control implants (Figure 3E).

Notch 1 and Notch 2 protein levels were significantly upregulated in implants with OP9-DL1, but Notch 4 expression level was distinctly decreased (Figure 3F). In addition, stimulation with the OP9-DL1 Notch ligand, caused rapid nuclear translocation of the cleaved domain of Notch 1 [16] and was widely detected in implants containing ECFC and OP9-DL1 (specific EC nuclear immunostaining for cleaved 1 [Val1744; Figure 3G]). This observation indicated that human ECFC-derived vessels were responsive to Dll1 ligand presentation *in vivo* and Notch 1 signaling was persistently activated in ECFC/OP9-DL1 implants *in vivo*. Also, anti-mouse smooth muscle α actin antibody staining (red) was detected in perivascular cells located around human ECFC-derived CD31$^+$ (brown) microvessels in co-implants with OP9-DL1 (Figure 3H). Together, these data suggest that Dll1 binding to Notch 1 significantly modulates vasculogenesis *in vivo* by inducing Notch signaling and promoting more ECFC-derived vessel formation with an overall enlarged vascular area and recruited host murine perivascular cells to the human vessels.

Dll1 expressed by OP9 stromal cells significantly reduces apoptosis of human CBECFCs in 3-dimensional collagen gels

To begin to understand the mechanisms through which Notch activation could enhance vasculogenesis of the human ECFC, we first examined whether the presence of OP9-DL1 co-implantation altered ECFC proliferation in the collagen gels and observed no effect (data not shown). We then tested whether the presence of OP9-DL1 decreases apoptosis of human CB ECFCs in the 3D collagen implants. After 1, 2, 3 or 5 days, the cells were recovered and assessed for apoptosis of ECFCs using AnnexinV and propidium iodide staining. Implanted ECFCs started undergoing apoptosis on day 1, and a significant majority of the cells died on day 2 and 3 after implantation (Figure 4A). We investigated whether a higher cell density of ECFC (3–6×10^6 cells/mL) might improve cell survival in the collagen gels and observed the increased cell density caused more apoptosis and no significant increase in vessel number or area (data not shown). In contrast, ECFC co-implanted with OP9-DL1 (1:1 cell ratio) revealed a significantly higher percentage of the AnnexinV$^-$/PI$^-$ viable cell population compared with ECFC alone or ECFC with OP9 implantation on day 1 and 3 (Figure 4B,C). These results indicated that co-implantation of ECFC with OP9-DL1 stromal cells increased survival of ECFC within the 3D collagen gels. Because caspase activation is a hallmark of apoptosis, we examined ECFC for evidence of caspase activation within the 3D gels. The caspase assay we used detected fluorescein-labeled inhibitors that bind to activated caspases 1 and 3/7 within cells. The inhibitors bind with 1:1 stoichiometry to the active centers of activated caspases. Thus, the assay can be used for quantitative analysis of the activated caspases in the cells. In every experiment performed, the caspase 3/7$^-$/PI$^-$ cell subset of ECFC co-implanted with OP9-DL1 was significantly higher on day 3 compared to implanted ECFC alone or ECFCs with OP9 implantation (Figure 4D). ECFC co-implanted with OP9-DL1 also displayed a greater percentage of caspase 1$^-$/PI$^-$ cells compared to ECFC alone or ECFC with OP9 implantation on day 2 and 3 (Figure 4E). These

observations indicate that Notch activation by OP9-DL1 stromal cells reduced activated caspase 3/7 and caspase 1 within ECFCs in collagen gels. Therefore, we conclude that Notch activation of ECFC in collagen gel implants enhanced survival of ECFCs by reducing activation of caspase 3/7 and caspase 1.

Discussion

Vasculogenesis is the process of primary capillary plexus formation from angioblasts during embryogenesis. Remodeling of the capillary plexus normally occurs via angiogenesis and arteriogenesis to form the hierarchical mature systemic vasculature [42,43]. It has been well established that Notch signaling plays an important role in regulating vascular patterning and remodeling during development [44–49] and after birth [7,24]. Previous studies in murine embryonic development showed that ectopic Notch 1 activation in ECs [45,46] caused vascular remodeling defects with enlarged vessel caliber. In contrast, small-sized vessels were present upon loss of active Notch signaling [46,47]. We report that the *in vivo* presence of stromal cell associated Notch ligand Dll1 led to enhanced vasculogenesis and vascular remodeling in human CB ECFCs, characterized by increased vessel density and enlarged vessel area (Figure 3). Accordingly, our observations coincide with the previous studies indicating that Dll1-dependent Notch 1 signaling regulates vessel size and state in murine embryogenesis.

A role for MSCs in promoting enhanced human ECFC vasculogenesis *in vivo* has been reported by several laboratories [50–57]. Indeed, conditioned medium secreted by multiple tissue–derived cultured MSCs promotes ECFC vasculogenesis *in vivo*, although the specific molecules promoting enhanced ECFC function remain elusive [55]. Surprisingly, we did not find a significant improvement in ECFC vasculogenic properties when the murine OP9 MSC were co-implanted with the ECFC in our studies. We speculate that differences in the types and composition of the 3D scaffolding proteins and strain of immunodeficient mice may play a role in the extent to which MSC promote human ECFC vasculogenesis *in vivo*. Although there are numerous matrices that permit ECFC and MSC, but not ECFC alone, to form vessels *in vivo* upon implantation into nude mice [52,58], CB ECFCs alone form human blood vessels in tissue engineered skin substitutes implanted in C.B-17 SCID/beige mice [59] or in type I collagen matrices implanted in NOD/SCID mice [26,27]. Further work to compare ECFC vasculogenesis directly in various matrices in several different immunodeficient murine hosts will be required to address the discrepancies in the literature.

VEGF plays a critical role in determining arterial-venous specification and the concentration of VEGF influences this determination [60]. In cultured murine ESCs, a high concentration of VEGF (50 ng/mL) drove an arterial-like endothelial gene expression pattern, whereas a low dose encouraged venous-like endothelial gene expression [60]. Similarly, addition of 100 ng/mL of rhVEGF-A to cultured cells upregulated an arterial-like endothelial gene expression pattern in hMAPCs and in hMSCs [61,62]. Recently, in the presence of 50 ng/mL of rhVEGF-A, arterial-like endothelial genes and downstream genes of Notch signaling were increased in cultured ECFCs [63]. The arterial-like endothelial genes induced by VEGF were decreased with treatment using γ-secretase inhibitor on cultured ECFCs [63]. This study indicated that VEGF-dependent induction leads to arterial-like gene expression with

Notch pathway signaling activation. Our results consistently confirmed previous work that rhVEGF-A at 50 ng/mL was sufficient to enhance expression of the arterial-like endothelial genes with activation of Notch in cultured CB ECFC (data not shown). In addition, Notch stimulated preconditioning *in vitro* was able to induce an arterial-like gene expression pattern *in vitro* (data not shown). However, preconditioning of ECFC *in vitro* with Notch stimulation failed to promote an arterial-like phenotype (data not shown) *in vivo*, suggesting that *in vitro* priming is not sufficient for *in vivo* specification in our experimental model. Of interest, *in vivo* co-implantation of OP9-DL1 stromal cells with ECFCs significantly enhanced vasculogenesis *in vivo* by promoting more ECFC-derived vessel formation with an overall enlarged vascular area and recruiting of murine perivascular cells around ECFC-derived vessels (Figure 3). Shepherd *et al.* [64] reported that co-implantation of human aortic smooth muscle cells promoted larger vessel size with periendothelial investment at 60 days post-implantation. Although we implanted the OP9-DL1 stromal cells with the ECFC, we observed an effect of Notch activation on human vessel size and recruitment of host perivascular cells. Future studies using specific perivascular cell subsets may indicate whether there are cell specific influences provided by different mesenchymal cell subsets on the human ECFC.

In the present work, implanted human CB ECFCs started undergoing apoptosis on day 1. After 2–5 days of implantation, most implanted ECFCs died with only 5–8% of total implanted cells persisting as perfused vessels (data not shown). Previous studies have indicated that human ECFC-lined vessels formed within subcutaneous implants in mice were found as early as day 1 or 2 following implantation, but these lumenized structures lacked significant perfusion with murine red blood cells at those early time points. However, ECFC-derived vessels perfused with host murine red blood cells (perfusion also confirmed by human specific lectin infusion and contrast-enhanced ultrasound flow detection) were detected after 3–4 days of implantation *in vivo* [52]. Thus, implanted endothelial cells had to survive at least 3–4 days *in vivo* to be able to contribute to a stable perfused capillary network. Given the proclivity of capillary networks to destabilize and regress with endothelial apoptosis in the absence of periendothelial support cells or adhesion of the endothelial cells to matrix proteins via cell surface integrin receptors [65–68], understanding the importance of a balance of pro-apoptotic versus anti-apoptotic signals in the plasticity of the capillary plexus has become an important paradigm. Perivascular support cells can induce endothelial cells to secrete basement membrane proteins that enhance endothelial cell integrin mediated attachment and increases in bcl-2 expression to protect cells from apoptosis [67,69]. HUVECs undergo apoptosis when implanted in immunodeficient mice within 24h, whereas Bcl-2 overexpression in HUVECs rescues them from apoptotic death and enhances the number and complexity of human vessels formed [70]. Bcl-2 overexpression in HUVECs also increases the number of human and mouse endothelial cell-lined vessels (vascularization) in implants and induces maturation of vessels by increasing tissue perfusion [59,71]. The frequency of the AnnexinV^{-}/PI^{-} viable cell population and overall hCD31^{+} vascular area in the ECFC/OP9-DL1 implants reflected a four-fold increase compared with the ECFC/OP9 implants (Figures 3E and 4C), suggesting a direct effect between diminishing apoptosis and increased vessel formation by Notch activation in ECFC *in vivo*. Our results suggest that improvement of cell survival of ECFCs by Dll1-dependent

Notch 1 signaling activation (Figure 3F) leads to vessel stabilization and promotes functional vessel formation in 3D collagen gels.

In summary, we have demonstrated that human CB ECFCs robustly form microvessels exhibiting a distinct remodeling pattern with increased vessel number and enlarged vessels by diminishing apoptosis of CB ECFCs during OP9-DL1 mediated Notch activation. Although other studies have shown that stromal cell co-implantation with ECFCs increases vessel number and maturation *in vivo* [53,72], we did not observe any enhancement of vasculogenesis by co-implanting ECFCs with OP9 stromal cells. However, co-implantation of OP9-DL1 led to constitutive ECFC Notch activation and resulted in greater numbers and maturation of human blood vessels *in vivo*. Further studies to present Notch activating ligands embedded within the matrix molecules may permit the modulation of human vessel formation using ECFC alone.

Supplementary Material

Refer to Web version on PubMed Central for supplementary material.

Acknowledgments

The authors thank Coleen P. Mallett for her help in isolation of human umbilical cord blood derived endothelial colony forming cells. This work was supported by funding from the Riley Children's Foundation.

References

1. Niessen K, Karsan A. Notch signaling in cardiac development. Circ Res. 2008; 102:1169–81. [PubMed: 18497317]
2. Radtke F, Fasnacht N, Macdonald HR. Notch signaling in the immune system. Immunity. 2010; 32:14–27. [PubMed: 20152168]
3. Ables JL, Breunig JJ, Eisch AJ, Rakic P. Not(ch) just development: Notch signalling in the adult brain. Nat Rev Neurosci. 2011; 12:269–83. [PubMed: 21505516]
4. Swift MR, Weinstein BM. Arterial-venous specification during development. Circ Res. 2009; 104:576–88. [PubMed: 19286613]
5. Kume T. Novel insights into the differential functions of Notch ligands in vascular formation. J Angiogenes Res. 2009; 1:8. [PubMed: 20016694]
6. Rocha SF, Adams RH. Molecular differentiation and specialization of vascular beds. Angiogenesis. 2009; 12:139–47. [PubMed: 19212819]
7. Takeshita K, Satoh M, Ii M, Silver M, Limbourg FP, Mukai Y, et al. Critical role of endothelial Notch1 signaling in postnatal angiogenesis. Circ Res. 2007; 100:70–8. [PubMed: 17158336]
8. Adams RH, Alitalo K. Molecular regulation of angiogenesis and lymphangiogenesis. Nat Rev Mol Cell Biol. 2007; 8:464–78. [PubMed: 17522591]
9. Alva JA, Iruela-Arispe ML. Notch signaling in vascular morphogenesis. Curr Opin Hematol. 2004; 11:278–83. [PubMed: 15314528]
10. Rossant J, Howard L. Signaling pathways in vascular development. Annu Rev Cell Dev Biol. 2002; 18:541–73. [PubMed: 12142271]
11. Shawber CJ, Kitajewski J. Notch function in the vasculature: insights from zebrafish, mouse and man. Bioessays. 2004; 26:225–34. [PubMed: 14988924]
12. Siekmann AF, Covassin L, Lawson ND. Modulation of VEGF signalling output by the Notch pathway. Bioessays. 2008; 30:303–13. [PubMed: 18348190]
13. Sorensen I, Adams RH, Gossler A. DLL1-mediated Notch activation regulates endothelial identity in mouse fetal arteries. Blood. 2009; 113:5680–8. [PubMed: 19144989]

14. Lawson ND, Vogel AM, Weinstein BM. sonic hedgehog and vascular endothelial growth factor act upstream of the Notch pathway during arterial endothelial differentiation. Dev Cell. 2002; 3:127–36. [PubMed: 12110173]
15. Zhong TP, Childs S, Leu JP, Fishman MC. Gridlock signalling pathway fashions the first embryonic artery. Nature. 2001; 414:216–20. [PubMed: 11700560]
16. Krebs LT, Xue Y, Norton CR, Shutter JR, Maguire M, Sundberg JP, et al. Notch signaling is essential for vascular morphogenesis in mice. Genes Dev. 2000; 14:1343–52. [PubMed: 10837027]
17. Huppert SS, Le A, Schroeter EH, Mumm JS, Saxena MT, Milner LA, et al. Embryonic lethality in mice homozygous for a processing-deficient allele of Notch1. Nature. 2000; 405:966–70. [PubMed: 10879540]
18. Jehn BM, Bielke W, Pear WS, Osborne BA. Cutting edge: protective effects of notch-1 on TCR-induced apoptosis. J Immunol. 1999; 162:635–8. [PubMed: 9916679]
19. Sade H, Krishna S, Sarin A. The anti-apoptotic effect of Notch-1 requires p56lck-dependent, Akt/PKB-mediated signaling in T cells. J Biol Chem. 2004; 279:2937–44. [PubMed: 14583609]
20. Beverly LJ, Felsher DW, Capobianco AJ. Suppression of p53 by Notch in lymphomagenesis: implications for initiation and regression. Cancer Res. 2005; 65:7159–68. [PubMed: 16103066]
21. MacKenzie F, Duriez P, Wong F, Noseda M, Karsan A. Notch4 inhibits endothelial apoptosis via RBP-Jkappa-dependent and -independent pathways. J Biol Chem. 2004; 279:11657–63. [PubMed: 14701863]
22. Ohishi K, Varnum-Finney B, Flowers D, Anasetti C, Myerson D, Bernstein ID. Monocytes express high amounts of Notch and undergo cytokine specific apoptosis following interaction with the Notch ligand, Delta-1. Blood. 2000; 95:2847–54. [PubMed: 10779430]
23. Liu ZJ, Shirakawa T, Li Y, Soma A, Oka M, Dotto GP, et al. Regulation of Notch1 and Dll4 by vascular endothelial growth factor in arterial endothelial cells: implications for modulating arteriogenesis and angiogenesis. Mol Cell Biol. 2003; 23:14–25. [PubMed: 12482957]
24. Limbourg A, Ploom M, Elligsen D, Sorensen I, Ziegelhoeffer T, Gossler A, et al. Notch ligand Delta-like 1 is essential for postnatal arteriogenesis. Circ Res. 2007; 100:363–71. [PubMed: 17234965]
25. Ingram DA, Mead LE, Tanaka H, Meade V, Fenoglio A, Mortell K, et al. Identification of a novel hierarchy of endothelial progenitor cells using human peripheral and umbilical cord blood. Blood. 2004; 104:2752–60. [PubMed: 15226175]
26. Huang L, Critser PJ, Grimes BR, Yoder MC. Human umbilical cord blood plasma can replace fetal bovine serum for in vitro expansion of functional human endothelial colony-forming cells. Cytotherapy. 2011; 13:712–21. [PubMed: 21250867]
27. Yoder MC, Mead LE, Prater D, Krier TR, Mroueh KN, Li F, et al. Redefining endothelial progenitor cells via clonal analysis and hematopoietic stem/progenitor cell principals. Blood. 2007; 109:1801–9. [PubMed: 17053059]
28. Mund JA, Estes ML, Yoder MC, Ingram DA Jr, Case J. Flow cytometric identification and functional characterization of immature and mature circulating endothelial cells. Arterioscler Thromb Vasc Biol. 2012; 32:1045–53. [PubMed: 22282356]
29. Hirschi KK, Ingram DA, Yoder MC. Assessing identity, phenotype, and fate of endothelial progenitor cells. Arterioscler Thromb Vasc Biol. 2008; 28:1584–95. [PubMed: 18669889]
30. Stump MM, Jordan GL Jr, Debakey ME, Halpert B. Endothelium grown from circulating blood on isolated intravascular Dacron hub. Am J Pathol. 1963; 43:361–7. [PubMed: 14057632]
31. Chen Y, Jacamo R, Shi YX, Wang RY, Battula VL, Konoplev S, et al. Human extramedullary bone marrow in mice: a novel *in vivo* model of genetically controlled hematopoietic microenvironment. Blood. 2012; 119:4971–80. [PubMed: 22490334]
32. Varnum-Finney B, Wu L, Yu M, Brashem-Stein C, Staats S, Flowers D, et al. Immobilization of Notch ligand, Delta-1, is required for induction of notch signaling. J Cell Sci. 2000; 23(113 Pt): 4313–8. [PubMed: 11069775]
33. Pfaffl MW. A new mathematical model for relative quantification in real-time RT-PCR. Nucleic Acids Res. 2001; 29:e45. [PubMed: 11328886]

34. Yang Z, Kondo T, Voorhorst CS, Nabinger SC, Ndong L, Yin F, et al. Increased c-Jun expression and reduced GATA2 expression promote aberrant monocytic differentiation induced by activating PTPN11 mutants. Mol Cell Biol. 2009; 29:4376–93. [PubMed: 19528235]
35. Schmitt TM, Zuniga-Pflucker JC. Induction of T cell development from hematopoietic progenitor cells by delta-like-1 in vitro. Immunity. 2002; 17:749–56. [PubMed: 12479821]
36. Critser PJ, Kreger ST, Voytik-Harbin SL, Yoder MC. Collagen matrix physical properties modulate endothelial colony forming cell-derived vessels *in vivo*. Microvasc Res. 80:23–30. [PubMed: 20219180]
37. Ingram DA, Mead LE, Moore DB, Woodard W, Fenoglio A, Yoder MC. Vessel wall-derived endothelial cells rapidly proliferate because they contain a complete hierarchy of endothelial progenitor cells. Blood. 2005; 105:2783–6. [PubMed: 15585655]
38. Duarte A, Hirashima M, Benedito R, Trindade A, Diniz P, Bekman E, et al. Dosage-sensitive requirement for mouse Dll4 in artery development. Genes Dev. 2004; 18:2474–8. [PubMed: 15466159]
39. Gale NW, Dominguez MG, Noguera I, Pan L, Hughes V, Valenzuela DM, et al. Haploinsufficiency of delta-like 4 ligand results in embryonic lethality due to major defects in arterial and vascular development. Proc Natl Acad Sci U S A. 2004; 101:15949–54. [PubMed: 15520367]
40. Lawson ND, Scheer N, Pham VN, Kim CH, Chitnis AB, Campos-Ortega JA, et al. Notch signaling is required for arterial-venous differentiation during embryonic vascular development. Development. 2001; 128:3675–83. [PubMed: 11585794]
41. Delaney C, Varnum-Finney B, Aoyama K, Brashem-Stein C, Bernstein ID. Dose-dependent effects of the Notch ligand Delta1 on *ex vivo* differentiation and *in vivo* marrow repopulating ability of cord blood cells. Blood. 2005; 106:2693–9. [PubMed: 15976178]
42. Carmeliet P. Mechanisms of angiogenesis and arteriogenesis. Nat Med. 2000; 6:389–95. [PubMed: 10742145]
43. Hanahan D. Signaling vascular morphogenesis and maintenance. Science. 1997; 277:48–50. [PubMed: 9229772]
44. Uyttendaele H, Ho J, Rossant J, Kitajewski J. Vascular patterning defects associated with expression of activated Notch4 in embryonic endothelium. Proc Natl Acad Sci U S A. 2001; 98:5643–8. [PubMed: 11344305]
45. Krebs LT, Starling C, Chervonsky AV, Gridley T. Notch1 activation in mice causes arteriovenous malformations phenocopied by ephrinB2 and EphB4 mutants. Genesis. 2010; 48:146–50. [PubMed: 20101599]
46. Copeland JN, Feng Y, Neradugomma NK, Fields PE, Vivian JL. Notch signaling regulates remodeling and vessel diameter in the extraembryonic yolk sac. BMC Dev Biol. 2011; 11:12. [PubMed: 21352545]
47. Benedito R, Trindade A, Hirashima M, Henrique D, da Costa LL, Rossant J, et al. Loss of Notch signalling induced by Dll4 causes arterial calibre reduction by increasing endothelial cell response to angiogenic stimuli. BMC Dev Biol. 2008; 8:117. [PubMed: 19087347]
48. Kim YH, Hu H, Guevara-Gallardo S, Lam MT, Fong SY, Wang RA. Artery and vein size is balanced by Notch and ephrin B2/EphB4 during angiogenesis. Development. 2008; 135:3755–64. [PubMed: 18952909]
49. Trindade A, Kumar SR, Scehnet JS, Lopes-da-Costa L, Becker J, Jiang W, et al. Overexpression of delta-like 4 induces arterialization and attenuates vessel formation in developing mouse embryos. Blood. 2008; 112:1720–9. [PubMed: 18559979]
50. Au P, Daheron LM, Duda DG, Cohen KS, Tyrrell JA, Lanning RM, et al. Differential *in vivo* potential of endothelial progenitor cells from human umbilical cord blood and adult peripheral blood to form functional long-lasting vessels. Blood. 2008; 111:1302–5. [PubMed: 17993613]
51. Au P, Tam J, Fukumura D, Jain RK. Bone marrow-derived mesenchymal stem cells facilitate engineering of long-lasting functional vasculature. Blood. 2008; 111:4551–8. [PubMed: 18256324]
52. Allen P, Kang K-T, Bischoff J. Rapid onset of perfused blood vessels after implantation of ECFCs and MPCs in collagen, PuraMatrix and fibrin provisional matrices. J Tissue Eng Reg. published online ahead of print August 16, 2013.

53. Melero-Martin JM, De Obaldia ME, Kang SY, Khan ZA, Yuan L, Oettgen P, et al. Engineering robust and functional vascular networks *in vivo* with human adult and cord blood-derived progenitor cells. Circ Res. 2008; 103:194–202. [PubMed: 18556575]
54. Traktuev DO, Prater DN, Merfeld-Clauss S, Sanjeevaiah AR, Saadatzadeh MR, Murphy M, et al. Robust functional vascular network formation *in vivo* by cooperation of adipose progenitor and endothelial cells. Circ Res. 2009; 104:1410–20. [PubMed: 19443841]
55. Lin RZ, Moreno-Luna R, Zhou B, Pu WT, Melero-Martin JM. Equal modulation of endothelial cell function by four distinct tissue-specific mesenchymal stem cells. Angiogenesis. 2012; 15:443–55. [PubMed: 22527199]
56. Wu X, Rabkin-Aikawa E, Guleserian KJ, Perry TE, Masuda Y, Sutherland FW, et al. Tissue-engineered microvessels on three-dimensional biodegradable scaffolds using human endothelial progenitor cells. Am J Physiol Heart Circ Physiol. 2004; 287:H480–487. [PubMed: 15277191]
57. Kang KT, Allen P, Bischoff J. Bioengineered human vascular networks transplanted into secondary mice reconnect with the host vasculature and re-establish perfusion. Blood. 2011; 118:6718–21. [PubMed: 22039257]
58. Allen P, Melero-Martin J, Bischoff J. Type I collagen, fibrin and PuraMatrix matrices provide permissive environments for human endothelial and mesenchymal progenitor cells to form neovascular networks. J Tissue Eng Regen Med. 2011; 5:e74–86. [PubMed: 21413157]
59. Shepherd BR, Enis DR, Wang F, Suarez Y, Pober JS, Schechner JS. Vascularization and engraftment of a human skin substitute using circulating progenitor cell-derived endothelial cells. FASEB J. 2006; 20:1739–41. [PubMed: 16807367]
60. Lanner F, Sohl M, Farnebo F. Functional arterial and venous fate is determined by graded VEGF signaling and notch status during embryonic stem cell differentiation. Arterioscler Thromb Vasc Biol. 2007; 27:487–93. [PubMed: 17185616]
61. Aranguren XL, Luttun A, Clavel C, Moreno C, Abizanda G, Barajas MA, et al. *In vitro* and *in vivo* arterial differentiation of human multipotent adult progenitor cells. Blood. 2007; 109:2634–42. [PubMed: 17090652]
62. Zhang G, Zhou J, Fan Q, Zheng Z, Zhang F, Liu X, et al. Arterial-venous endothelial cell fate is related to vascular endothelial growth factor and Notch status during human bone mesenchymal stem cell differentiation. FEBS Lett. 2008; 582:2957–64. [PubMed: 18671974]
63. Boyer-Di Ponio J, El-Ayoubi F, Glacial F, Ganeshamoorthy K, Driancourt C, Godet M, et al. Instruction of circulating endothelial progenitors in vitro towards specialized blood-brain barrier and arterial phenotypes. PLoS One. 2014; 9:e84179. [PubMed: 24392113]
64. Shepherd BR, Jay SM, Saltzman WM, Tellides G, Pober JS. Human aortic smooth muscle cells promote arteriole formation by coengrafted endothelial cells. Tissue Eng Part A. 2009; 15:165–73. [PubMed: 18620481]
65. Fukai F, Mashimo M, Akiyama K, Goto T, Tanuma S, Katayama T. Modulation of apoptotic cell death by extracellular matrix proteins and a fibronectin-derived antiadhesive peptide. Exp Cell Res. 1998; 242:92–9. [PubMed: 9665806]
66. Brooks PC, Montgomery AM, Rosenfeld M, Reisfeld RA, Hu T, Klier G, et al. Integrin alpha v beta 3 antagonists promote tumor regression by inducing apoptosis of angiogenic blood vessels. Cell. 1994; 79:1157–64. [PubMed: 7528107]
67. Pollman MJ, Naumovski L, Gibbons GH. Endothelial cell apoptosis in capillary network remodeling. J Cell Physiol. 1999; 178:359–70. [PubMed: 9989782]
68. Stratman AN, Schwindt AE, Malotte KM, Davis GE. Endothelial-derived PDGF-BB and HB-EGF coordinately regulate pericyte recruitment during vasculogenic tube assembly and stabilization. Blood. 2010; 116:4720–30. [PubMed: 20739660]
69. Stromblad S, Becker JC, Yebra M, Brooks PC, Cheresh DA. Suppression of p53 activity and p21WAF1/CIP1 expression by vascular cell integrin alphaVbeta3 during angiogenesis. J Clin Invest. 1996; 98:426–33. [PubMed: 8755653]
70. Zheng L, Dengler TJ, Kluger MS, Madge LA, Schechner JS, Maher SE, et al. Cytoprotection of human umbilical vein endothelial cells against apoptosis and CTL-mediated lysis provided by caspase-resistant Bcl-2 without alterations in growth or activation responses. J Immunol. 2000; 164:4665–71. [PubMed: 10779771]

71. Enis DR, Shepherd BR, Wang Y, Qasim A, Shanahan CM, Weissberg PL, et al. Induction, differentiation, and remodeling of blood vessels after transplantation of Bcl-2-transduced endothelial cells. Proc Natl Acad Sci U S A. 2005; 102:425–30. [PubMed: 15625106]

72. Melero-Martin JM, De Obaldia ME, Allen P, Dudley AC, Klagsbrun M, Bischoff J. Host myeloid cells are necessary for creating bioengineered human vascular networks *in vivo*. Tissue Eng Part A. 2010; 16:2457–66. [PubMed: 20218762]

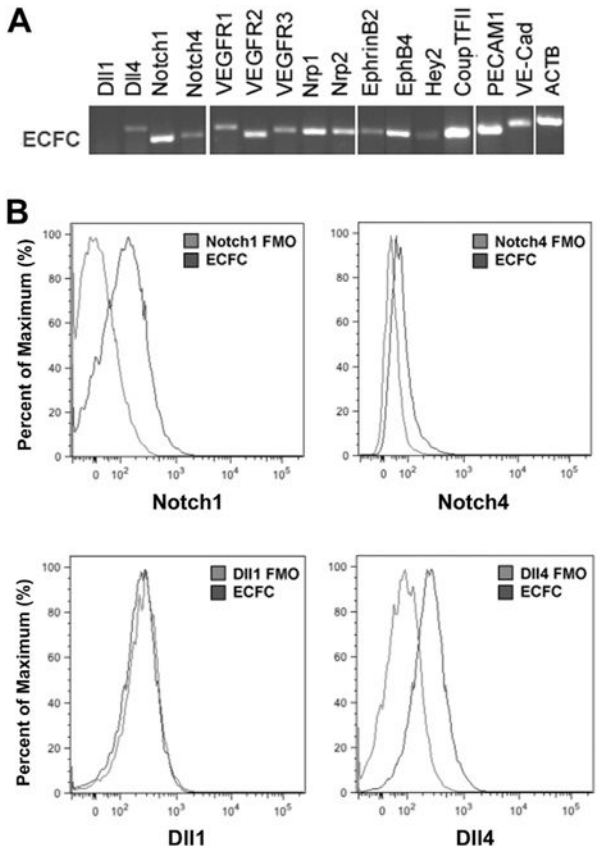

Figure 1.

The expression of Notch pathway related transcripts in cultured ECFCs. (A) Human CB–derived ECFCs expressed numerous Notch pathway related transcripts and EC gene markers such as platelet endothelial cell adhesion molecule-l and VE-Cadherin. (B) Notch ligands and receptors were expressed on a subset of ECFCs. The representative histograms show comparison between fluorescence minus one (FMO) control (gray) and Notch molecule expression (black) on the surface of ECFCs.

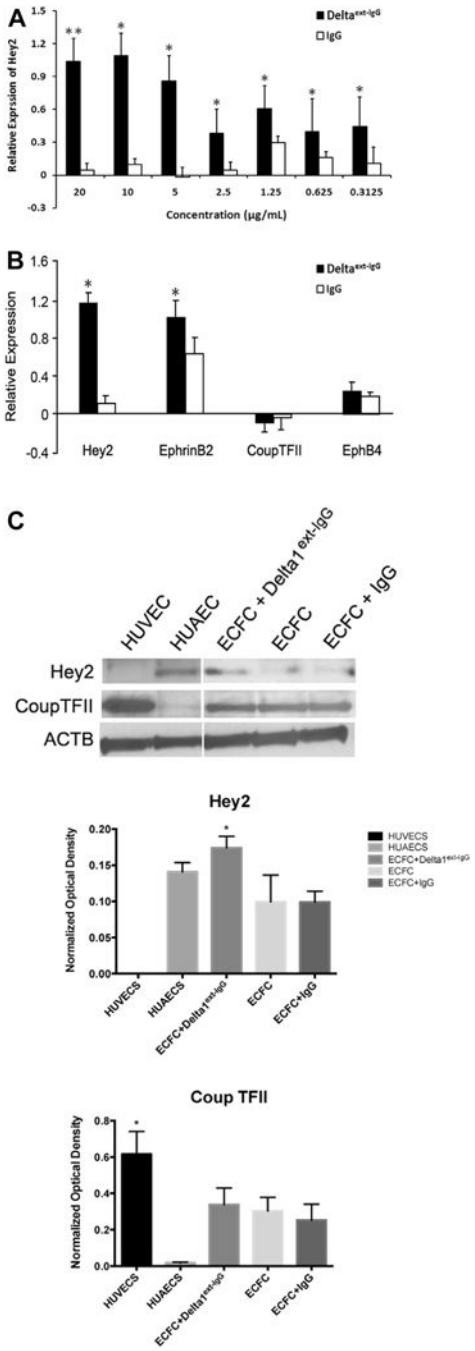

Figure 2.

ECFCs respond to Notch signaling with increased expression of known downstream target genes (n = 3). The dose-dependent activation of endogenous Notch signaling in human CB–derived ECFCs is indicated by Hey2 (A) expression after 3 days of incubation in various concentrations of Delta$^{1ext\text{-}IgG}$. (B) Quantitative RT-PCR analysis revealed Hey2 and EphrinB2 transcripts were significantly increased after 3 days of stimulation with 10 μg/mL Delta 1$^{ext\text{-}IgG}$, whereas the expression of Coup TFII and EphB4 were not significantly affected. Expression levels were presented as a fold change (in logarithmic scale) compared

with baseline levels and were normalized by using ATP5B as a housekeeping gene. The expression at day 0 in nontreated cells served as a baseline value. n = 5. *$P < 0.05$. (C) Upper panel depicts representative immunoblots of Hey2 and Coup TFII proteins and lower panel reveals quantification (protein expression levels were normalized by using β-actin). *$P < 0.05$. HUAEC, human umbilical artery endothelial cells; HUVEC, human umbilical vein endothelial cells.

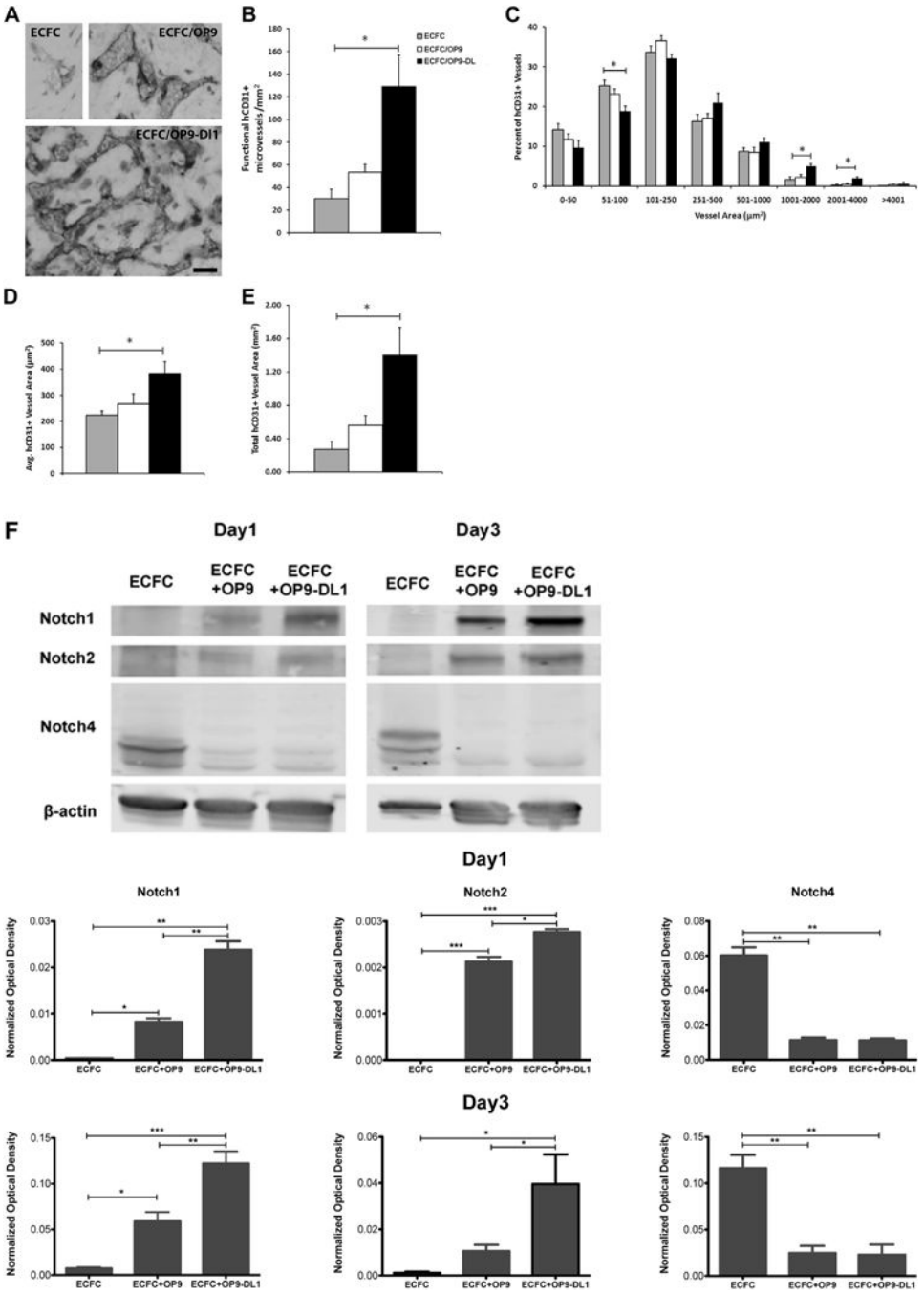

Figure 3a

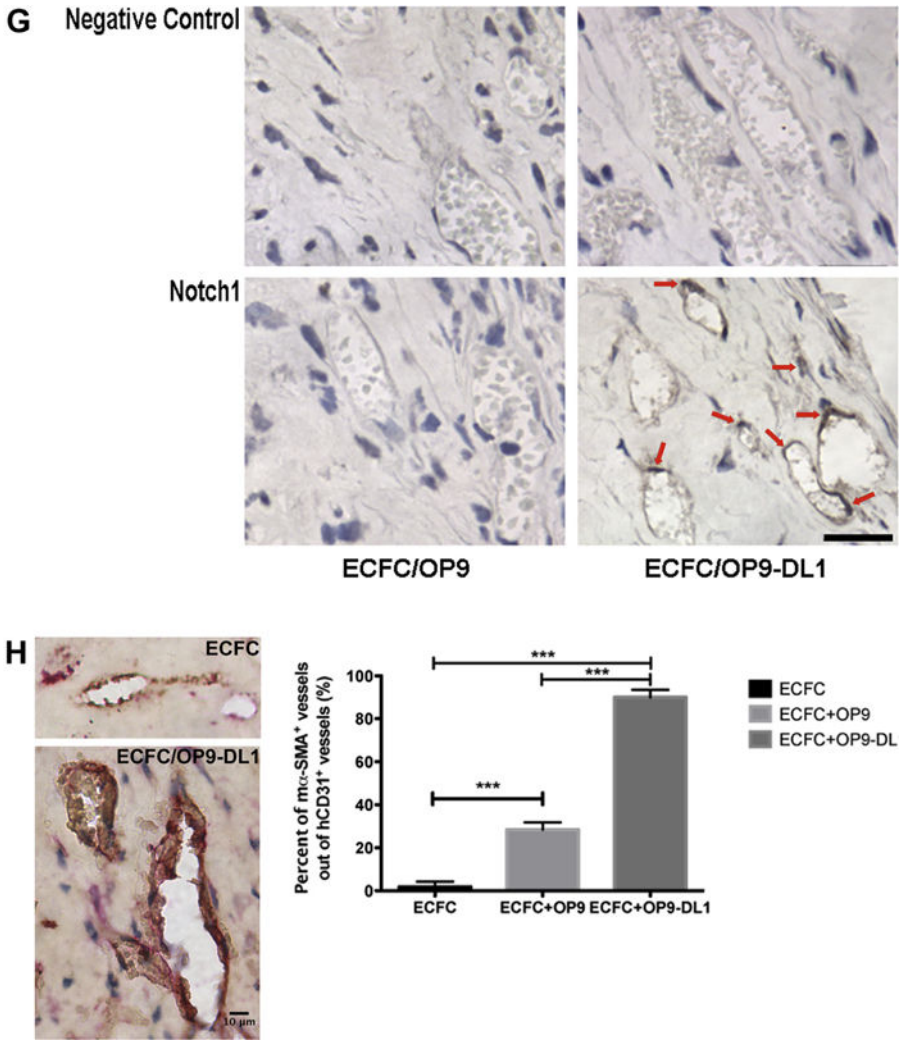

Figure 3b

Figure 3.

In vivo Dll1 stimulation boosts the formation of functional vessels (n = 3). (A) Anti-human CD31 staining identified human CB–derived ECFCs, alone or combined with OP9 or OP9-DL1, that have formed microvessels in collagen gels after 14 days of implantation. Upon the stimulation of Dll1, there was a significant increase in the number of vessels formed by human CB–derived ECFCs and perfused with murine red blood cells per mm^2 in the gel (B). In addition, the size distribution of hCD31+ microvessels was noticeably altered (C), shifting toward larger-sized vessels (1001–4000 μm^2) with Dll1 stimulation. Moreover, vessel morphology was significantly altered by the presence of Dll1 with increased average vessel area (D) and total vascular areas (E). (F) Upper panel shows representative immunoblots of Notch 1, Notch 2 and Notch 4 proteins and lower 2 panels show quantification of repeated experiments (protein expression levels were normalized using β-actin); n = 3. $*P < 0.05$. Anti-cleaved Notch 1 (Val1744) antibody staining (G) in endothelial nuclei confirms that the activation of Notch 1 is detected *in vivo* in newly formed human vessels in the presence of Dll1; n = 6. Scale bar represents 100 μm. (H) Anti-mouse smooth

muscle α actin (αSMA) antibody staining (red) was detected in perivascular cells around human ECFC–derived $CD31^+$ vessels (brown) in implants with OP9-DL1 stromal cells. Scale bar represents 10 μm. *$P < 0.05$; **$P < 0.001$; ***$P < 0.0001$.

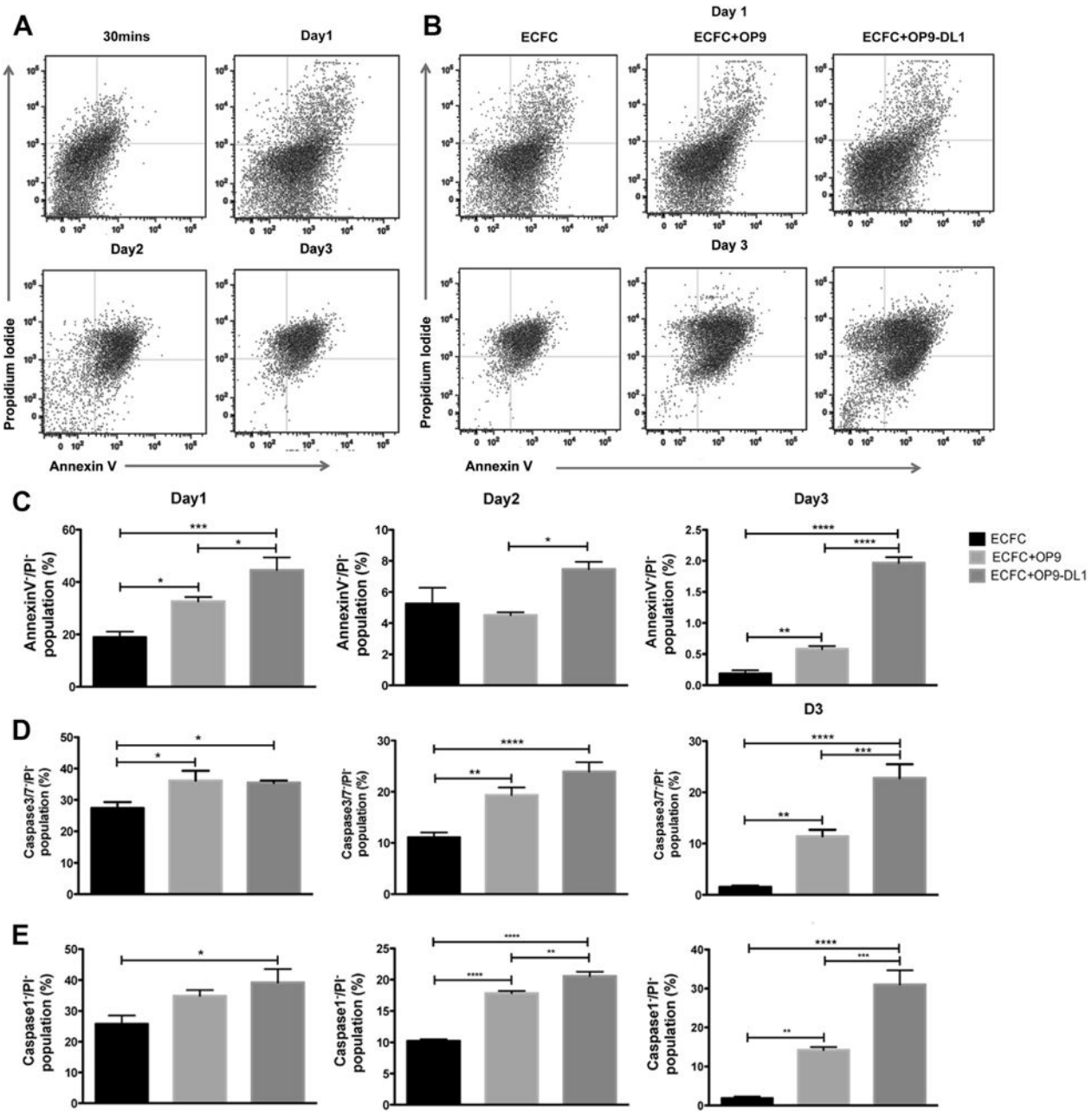

Figure 4.

OP9-DL1 stimulation diminishes apoptosis of ECFCs in collagen gels (n = 5). (A) Representative dot plots of apoptosis analysis of ECFCs at 30 min or on days 1–3. (B) Representative dot plots of apoptosis analysis of ECFC alone, co-implanted with OP9, or OP9-DL1 on days 1–3. (C) The Annexin^{-}/PI^{-} viable population of ECFC co-implanted with OP9-DL1 was significantly higher on day 1 and 3 compared with implantation of ECFC alone or ECFC with OP9 on day 1 and 3. (D) The percentage of the Caspase 3/7^{-}/PI^{-} population of ECFC co-implanted with OP9-DL1 was significantly greater compared with ECFC alone or with OP9 on day 3. (E) ECFC co-implanted with OP9-DL1 displayed a

higher percentage of Caspase $1^{-}/PI^{-}$ cells compared with ECFC alone or ECFC with OP9 co-implants. n = 6. $*P < 0.05$.

Table I

Primers used for conventional RT-PCR.

Gene	Forward	Reverse	Tm	Product size (bp)
VEGFR1	AGTTTAAAAGGCACCCAGCA	ACGAGCTCCCTTCCTTCAGT	55	362
VEGFR2	GAGGGACTTGGACTGGCTTT	GATTTGAAATGGACCCGAGA	55	302
VEGFR3	TGAACATCACGGAGGAGTCA	TCAGGCTTGTTGATGAATGG	55	337
NRP1	GAAAAATGCGAATGGCTGAT	AATCCGGGGGACTTTATCAC	53	335
NRP2	CAAACACTGTGGGAACATCG	TGTCCAGCCAATCGTACTTG	55	338
DLL1	TGTGCCTCAAGCACTACCAG	ACACACGAAGCGGTAGGAGT	55	353
DLL4	TATTGGGCACCAACTCCTTC	ACATAGTGGCCGAAGTGGTC	55	349
NOTCH 1	GGCCAGAACTGTGAGGAAAA	GCAGTAGAAGGAGGCCACAC	57	327
NOTCH 4	TCTCCCTCTCCATTGACACC	TGGAAGCACTCGTTGACATC	55	323
HEY2	TGGGGAGCGAGAACAATTAC	GCACTCTCGGAATCCTATGC	55	329
EFNB2 (C)	TTATTTGCCCCAAAGTGGAC	CCTGGTTGATCCAGCAGAAC	55	347
EPHB4	GAGCTGTGTGGCAATCAAGA	ACTTTGCAGACGAGGTTGCT	55	345
COUP TFII	AACACATCGAGTGCGTGGT	CAGGTACGAGTGGCAGTTGA	55	311
PECAM1	GCAAAATGGGAAGAACCTGA	ACAGTTGACCCTCACGATCC	55	316
VECAD	TGGACAAGGACACTGGTGAA	TCTTGCAGAGTGACCAGCAC	55	382
ACTB	GCCAGCTCACCATGGATGAT	GTCTCAAACATGATCTGGGTC	57	388

Table II

Primers used for quantitative RT-PCR.

Gene	Forward	Reverse	Eff
VEGFR1	GCTTCTGACCTGTGAAGCAA	CTCGTGTTCAAGGGAGTGGT	1.987
VEGFR2	GAACATTTGGGAAATCTCTTGC	CGGAAGAACAATGTAGTCTTTGC	1.917
VEGFR3	AGACAAGAAAGCGGCTTCAG	TTGGGAGTCAGGGTGTGC	1.860
NRP1	GTTGTGTCTTCAGGGCCATT	AATCCGGGGGACTTTATCAC	2.036
NRP2	TCTGCGCTACGAGATCTTCA	GTGCAGTCCAAGTTGTGTGG	1.862
DLL4	GACCACTTCGGCCACTATGT	TTGCTGCAGTAGCCATTCTG	1.967
NOTCH 1	CTTCAATGACCCCTGGAAGA	GAAGTGGAAGGAGCTGTTGC	1.950
NOTCH 4	CTGCTGCTGCTGCTATGTGT	GTCAGGAAACTGGCACGTCT	1.833
HES1	TGCTTCACTGTCATTTCCAGA	GAAAGTCTGAGCCAGCTGAA	1.958
HEY2	CTTGTGCCAACTGCTTTTGA	TCATGAAGTCCATGGCAAGA	1.912
EFNB2	TCTTTGGAGGGCCTGGAT	CCAGCAGAACTTGCATCTTG	1.986
EPHB4	TTTGGCTCCTTCGAGCTG	GGCCAAGATTTTCTTCTGGTG	1.880
COUP TFII	CCAAGAGCAAGTGGAGAAGC	TCCACATGGGCTACATCAGA	1.988
ATP5B	CCACTACCAAGAAGGGATCTATCA	GGGCAGGGTCAGTCAAGTC	1.960